

# Glass transition, thermal stability and glass-forming tendency of $\text{Se}_{85}\text{Te}_{10}\text{X}_5$ ( $\text{X} = \text{In}, \text{Sn}$ ) chalcogenide glasses

A.S.Farid, N.A.Hegab, E.Abd El-Wahabb and H.Magdy

**Abstract**— Bulk glasses of compositions  $\text{Se}_{85}\text{Te}_{10}\text{X}_5$  ( $\text{X} = \text{In}, \text{Sn}$ ) prepared by melt quenching technique. These samples were structurally characterized using X-ray diffraction. Kinetics of phase transformations of  $\text{Se}_{85}\text{Te}_{10}\text{X}_5$  ( $\text{X} = \text{In}, \text{Sn}$ ) glassy compositions have been studied using differential thermal analysis (DTA) under non-isothermal conditions at five different heating rates ( $\alpha = 10, 20, 30, 40$  and  $50^\circ \text{C/min}$ ). From the heating rate dependence of glass transition temperature  $T_g$  and peak crystallization temperature  $T_p$ , the activation energy of glass transition  $E_g$ , the activation energy of crystallization  $E_c$ , the order parameter ( $n$ ), the dimensionality of growth and the frequency factor  $k_o$  determined via three models; Kissinger, Augis-Bennett and Mahadevan et al. According to Avrami index  $n$ , the crystallization mechanism was interpreted as three-dimensional growth for  $\text{Se}_{85}\text{Te}_{10}\text{Sn}_5$  and two-dimensional growth for  $\text{Se}_{85}\text{Te}_{10}\text{In}_5$  composition. Some kinetic parameters; the Hruby number  $H_r$ , the glass formation ability (GFT), the temperature difference ( $T_c - T_g$ ), the reduced glass transition temperature  $T_{rg}$  and the thermal stability  $S$  studied as functions of heating rates and compositions.

**Index Term**— Chalcogenide glasses, Chalcogenide material, Crystal growth, Crystallization approximation models, Differential thermal analysis, Glass activation energy, Stability parameter.

## 1 INTRODUCTION

Chalcogenide glasses are interesting materials belonging to the inorganic disordered solids. These glasses are subjects of intense research both for basic physics understanding as well as targets for device fabrication owing to their easily modifiable electrical, optical and thermal properties. Se-based chalcogenide alloys are the most materials in terms of composition and preparative conditions, and have wide potential for technological applications in solid state devices. Applications include xerography, reversible optical recording and electrical memory and threshold switching [1], [2], [3]. Amorphous selenium assumed to consist of two structural arrangements, long chains and  $\text{Se}_8$  rings in a mixture held by presumably weak Van der Waal's forces with strong covalent bonding between the atoms in the chains or rings [4]. These molecular bonds imply that these glasses are less robust and mechanically weaker than oxide glasses. Moreover, the amorphous phase of Se is associated with a short lifetime, low sensitivity (nucleation and crystallization rates) and low thermal stability and thus poses limited applications. Additives are significant in increasing thermal stability, sensitivity, thermal and electrical conductivity, lifetime and glass transition temperature.

Amorphous Se-Te alloys have greater hardness, higher photosensitivity and smaller aging effects than pure Se. As these glasses have poor thermo-mechanical properties, in

order to enlarge their domain of applications, it is necessary to increase their softening temperature and mechanical strength. The effect of addition of third element (In, Sn or Sb) into Se-Te glass has been carried out many research groups [5], [6], [7], [8], [9], [10], [11], [12]. The addition of indium (In) which has a large electronegativity difference with Se and Te, expands the glass forming area and also creates compositional and configurational disorder in the system, and also is found to modify the structure and thus the electrical and thermal properties of the Se-Te system [13], [14], [15], [16], [17]. The addition of impurities like Sn is particularly of much interest as it has produced a remarkable change in the optical, electrical and thermal properties of chalcogenide glasses. The lattice perfection and the optical gap of the material play a major role in the preparation of the device which modified by the addition of the dopant (Sn).

There are two methods can be used to study the crystallization kinetics in chalcogenide glasses: isothermal and non-isothermal methods. In the isothermal method, the sample is brought near to the crystallization temperature very quickly and then any physical quantity change drastically is measured as a function of time. In the non-isothermal method, the sample heated at a fixed rate and physical parameter recorded as a function of temperature. We use the non-isothermal method because the measurements made in a relatively rapid and precise manner. The aim of the present work is to analyze the glass transition and crystallization kinetics of amorphous  $\text{Se}_{85}\text{Te}_{10}\text{X}_5$  ( $\text{X} = \text{In}, \text{Sn}$ ) compositions by means of non-isothermal differential thermal analysis (DTA) measurements at different heating rates using three different methods of analysis namely, Kissinger's relation [18], Matusita-Sakka theory [19] and Augis-Bennett approximation [20].

- A.S.Farid, Physics Department, Faculty of Education, Ain Shams University, Cairo, Egypt. E-mail: abir\_net\_2005@hotmail.com
- N.A.Hegab, Physics Department, Faculty of Education, Ain Shams University, Cairo, Egypt. E-mail: drnaemahegab@yahoo.com
- E.Abd El-Wahabb, Physics Department, Faculty of Education, Ain Shams University, Cairo, Egypt. E-mail: e\_wahabb@hotmail.com

## 2 EXPERIMENTAL TECHNIQUES

Samples of  $Se_{85}Te_{10}X_5$  ( $X = In, Sn$ ) glassy system prepared in bulk form by melt quenching technique. For each sample, materials of 99.999% purity weighed according to their atomic percentage are sealed in evacuated quartz ampoules ( $\sim 10^{-5}$  Torr). The sealed ampoules were then heated to  $\sim 1273$  K in an oscillatory furnace at a heating rate of 3K/min and were frequently rocked for about 10 hours at the highest temperature to make the melt homogenous. The quenching has done in ice-cooled water. The structure of the investigated samples was examined by X-ray diffraction analysis (Shimadzu XD-D2) with Cu target and Ni filter. The chemical composition of the obtained samples is checked by energy dispersive X-ray analysis using a scanning electron microscope (Joel 5400). Fully quantitative analysis of the results has obtained from the spectra by processing the data through ZAF correction program. The samples so obtained were ground to powder form for carrying out DTA measurements. The thermal behavior was investigated using a differential thermal analyzer (Shimadzu DTA-50). Five heating rates ( $\alpha = 10, 20, 30, 40$  and  $50^\circ\text{C}/\text{min}$ ) were selected for DTA measurements. About  $10^{-15}$  mg. powder, heated at constant heating rate and the changes in heat flow with reference to empty reference pan were measured. The presence of a well-defined endothermic peak (at the glass transition temperature and melting temperature) and an exothermic peak (at the crystallization temperature) was observed in each DTA analysis.

## 3 RESULTS AND DISCUSSION

### 3.1.1 Structural and thermal analysis

X-ray diffraction was carried out for the investigated samples of  $Se_{85}Te_{10}X_5$  ( $X$  stands for In or Sn). The obtained X-ray patterns for the studied samples shown in Fig.1. The absence of any sharp peak confirms the amorphous nature of these samples.

### 3.1.2 Energy dispersive X-ray spectrum analysis EDX

Composition of the investigated samples was checked by energy dispersive X-ray spectrum analysis using a scanning electron microscope. The obtained data showed that the percentage of the constituent elements of the studied samples are approximately the same as given in Table 1.

### 3.1.3 Differential thermal analysis DTA

The phase transformation of the samples observed through DTA at five different heating rates ( $\alpha = 10, 20, 30, 40$  and  $50^\circ\text{C}/\text{min}$ ). A typical DTA thermogram of  $Se_{85}Te_{10}In_5$  and  $Se_{85}Te_{10}Sn_5$  glassy samples at heating rate  $10^\circ\text{C}/\text{min}$  as representative examples shown in Figs.2 (a, b). When the sample heated at a constant heating rate in differential thermal analysis experiment, the glass undergoes structural changes. The DTA traces show three characteristic phenomena. The first one is an endothermic region which denoting as glass transition region while the second is an exothermic phenomenon manifesting the crystallization process and the last is an endothermic phenomenon corresponding to the melting point of the sample.

The glass transition is generally considered to occur due to changes in the amorphous structure. The DTA traces of the studied samples show single glass transition peak  $T_g$  and which confirms

the homogeneity of the samples. In addition, the glass transition temperature  $T_g$  represents the strength or rigidity of the glassy alloy [21], [22]. Also, there is an exothermic peak originating which arises due to an abrupt increase in specific heat of the sample.

From the Amorphous- Crystallization Transformation, this exothermic peak has three characteristic points, The first point is the onset temperature of crystallization  $T_i$ , the second is the peak temperature  $T_p$  and the third is the final temperature of crystallization  $T_f$ .

Fig.2 shows the characteristic melting temperature  $T_m$  represented by an endothermic peak. Tables 2& 3 illustrate the values of  $T_g$ ,  $T_p$  and  $T_m$  for the studied compositions at different heating rates as mentioned above. It is clear from these tables that  $T_g$ ,  $T_p$  and  $T_m$  increase with increasing heating rates for the studied compositions. The  $T_g$  of multi-component glass is known to be dependent on several independent parameters such as band gap, coordination numbers, bond energy, effective molecular weight and the type and fraction of various structural units formed [23], [24], [25].

It is clear from Tables 2& 3 that  $T_g$  for  $Se_{85}Te_{10}Sn_5$  is lower than that for  $Se_{85}Te_{10}In_5$ . This understood according to the chemical bond energies given in Table 4 between the constituent elements in the investigated samples [26]. Since the Se - In bond ( $183.86$  kJ/mol) is higher than that of Se - Sn ( $176.65$  kJ/mol). This increase of  $T_g$  with addition of In attributed to the cross linking of Se - Te chains and substitution of Se - Se homopolar bonds with Se - In heteropolar bonds with increased bond energy as mentioned above. Consequently increases the overall cohesive energy of the system which in turns increases the glass transition temperature ( $T_g$ ). This will lead to increase the lattice rigidity as well as  $T_g$  and decrease the thermal stability as well as  $T_p$  [21].

### 3.2 Kinetics of phase transformation

#### 3.2.1 glass transition region

The dependence of glass transition temperature  $T_g$  on the heating rate  $\alpha$  used to study the glass transformation region of a material and determine the value of activation for glass transition  $E_g$ .

The kinetics of glass transition can be studied using the dependence of  $T_g$  on the heating rate  $\alpha$ . This dependence discussed on the base of three approaches.

**The first one is corresponding to the empirical relation suggested by losaka [27] in the form:**

$$T_g = A + B \ln \alpha \quad (1)$$

where A and B are constants. The value of constant A indicates the glass transition temperature for the heating rate of 1K/min, while the value of constant B is dependent on the glass composition [27] and the cooling rate of the melt: the lower cooling rate of the melt, the lower value of B. The plot of  $T_g$  versus  $\ln \alpha$  for the glassy compositions shown in Fig.4. The values of A and B for the studied compositions given in Table 5. The values of A and B are in agreement with that obtained before [28], [29].

**The second approach is the use of Kissinger formulation [30] to show the dependence of  $T_g$  on heating rate and then evaluation of**

the activation energy for glass transition  $E_g$ . In spite of the fact that the Kissinger equation is basically derived for the determination of activation energy of crystallization process ( $E_c$ ), it is shown [31-34] that the same equation can be used for evaluation of the glass transition activation energy ( $E_g$ ).

According to Kissinger, the value of ( $E_c$ ) can be determined from the formula [26]:

$$\ln(\alpha / T_g^2) = -(E_c / RT_g) + \text{cons} \quad (2)$$

where  $E_c$  is the activation energy for crystallization and  $R$  is the universal gas constant ( $R = 8.3144 \text{ J/mol}$ ).

Equation (2) can be used to calculate the value of  $E_g$ ; i.e. replacing  $T_p$  by  $T_g$  and  $E_c$  by  $E_g$  where the above equation takes the following form for the glass transition kinetics

$$\ln(\alpha / T_g^2) = -(E_g / RT_g) + \text{cons} \quad (3)$$

Eq. (3) states that  $\ln(\alpha / T_g^2)$  versus  $(1000 / T_g) \text{ K}^{-1}$  plot should be straight line as shown in Fig.5 for the studied samples. The values of  $E_g$  deduced from the slope of Fig.5 according to Eq. (3) and listed in Table 5.

**The third approximation of Mahadevan et al.** [35] where the variation of  $\ln(1/T_g^2)$  with  $\ln \alpha$ . Thus, the Kissinger equation can be simplified to

$$\ln \alpha = -(E_g / RT_g) + \text{cons} \quad (4)$$

A plot of  $\ln \alpha$  against  $(1000 / T_g) \text{ K}^{-1}$  for the studied compositions shown in Fig.6. Values of the activation energy are obtained from the slope of the resulting straight lines in Fig.6 and listed in Table 5.

It is apparent from this table that the deduced values of  $E_g$  based on the three models are in agreement with each other. This means that any of the three methods is suitable for calculating the glass transition activation energy.

The glass transition activation energy defined as the amount of energy that absorbed by a group of atoms in the glassy region, so a jump from one metastable to another is possible [36].  $E_g$  involved in the molecular motions and the rearrangement of atoms around the glass transition temperature [37].

It is clear from Table 5 that the values of  $E_g$  for  $\text{Se}_{85}\text{Te}_{10}\text{In}_5$  composition is lower than that for  $\text{Se}_{85}\text{Te}_{10}\text{Sn}_5$  composition: that is due to the higher internal energy with In addition than Sn addition to Se -Te system, Hence the probability of atom jump to the lower energy metastable states decreases with In addition than Sn addition to Se - Te system.

### 3.2.2 Crystallization kinetics, activation energy and dimensionality of growth.

In this section, three different approaches [30], [38], [39] concerning the kinetics analysis of crystallization reaction and the temperature dependence of the reaction rate constant. It has pointed out [30] that in a crystallization process, three types of activation energies have to be involved: activation energy for nucleation, activation energy for growth and activation energy  $E_c$  for the whole crystallization process. Various studies [35], [38], [39] show that the activation energy for growth may be taken equal to

the activation energy of the whole crystallization  $E_c$  provided it is evaluated using thermal analysis of the sample. The following methods have been used to estimate the activation energy for crystallization.

#### 3.2.2.1 Kissinger model

The evaluation of the activation energy for crystallization  $E_c$  from the variation of the peak temperature  $T_p$  with heating rate ( $\alpha$ ) undertaken by using the Kissinger equation Eq.(2) [25]. Fig.7 shows the plot of  $\ln(\alpha / T_p^2)$  against  $(1 / T_p)$  for the studied samples. The data fitted by straight lines. The slope of the plot gives the activation energy  $E_c$ . The obtained values of  $E_c$  listed in Table 6 for the studied samples.

#### 3.2.2.2 Augis and Bennett model

The activation energy ( $E_c$ ) of crystallization can be deduced from the approximation method advanced by Augis and Bennett [20] which follows the expression:

$$\ln[\alpha / (T_p - T_o)] = -(E_c / RT_p) + \ln k_o \quad (5)$$

where  $T_o$  is the initial temperature and  $k_o$  is the frequency of attempts made by the nuclei to overcome the energy barrier during crystallization. In case of  $T_p > T_o$  the previous relation can be approximated as follows:

$$\ln(\alpha / T_p) = -(E_c / RT_p) + \ln k_o \quad (6)$$

From this approximation values of  $E_c$  can be obtained from the slope of the linear plots shown in Fig.8 of  $\ln(\alpha / T_p)$  and  $(1000 / T_p) \text{ K}^{-1}$  for the studied samples. The y-intercept of the obtained straight lines corresponding to  $\ln k_o$  from which the frequency factor obtained. The obtained values of  $E_c$  and  $k_o$  listed in Tables 6 and 7. It is observed that the value of the frequency factor  $k_o$  is lower with In addition than Sn addition.

This indicates that  $\text{Se}_{85}\text{Te}_{10}\text{In}_5$  has greater crystalline tendency than  $\text{Se}_{85}\text{Te}_{10}\text{Sn}_5$ .

#### 3.2.2.3 Mahadevan et al. model

The activation energy  $E_c$  of crystallization can be also calculated from the variation of the peak crystallization temperature  $T_p$  with the heating rate through the use of an approximation developed by Mahadevan et al. based on the following equation:

$$\ln \alpha = -(E_c / RT_p) + \text{cons} \quad (7)$$

The plot of  $\ln \alpha$  against  $(1000 / T_p) \text{ K}^{-1}$  yields a straight line, the slope of which gives the activation energy of crystallization  $E_c$ . Fig.9 shows the plots for  $\text{Se}_{85}\text{Te}_{10}\text{In}_5$  and  $\text{Se}_{85}\text{Te}_{10}\text{Sn}_5$  from which  $E_c$  values are come out and given in Table 6.

From Table 6, It is clear that the barrier to crystallization for  $\text{Se}_{85}\text{Te}_{10}\text{In}_5$  is higher than that for  $\text{Se}_{85}\text{Te}_{10}\text{Sn}_5$  sample. This indicates that the atoms require large energy to jump from the glassy state to the crystalline state. The difference in the activation energy as calculated with the different models, even for the same sample, may be attributed to the different approximations used in the models.

#### 3.2.2.4 Matusita and Sakka model

Matusita et al. [19] suggested an equation, which is applicable for kinetic of crystallization under non-isothermal conditions and given as



$$\ln[-\ln(1-\chi)] = -n \ln \alpha - 1.052mE_c / RT + \text{cons} \quad (8)$$

where  $\chi$  is the volume of the fraction crystallize at any temperature  $T$ , and given by  $\chi = (A_T/A)$  where  $A_T$  is the area between  $T_i$  and  $T$  as shown by the hatched portion in Fig.2,  $A$  is the total area of the exothermic peak between the temperature  $T_i$  where the crystallization just begins and the temperature  $T_f$  where the crystalline state completed,  $m$  and  $n$  are constants related to the crystallization mechanism. For a quenched glass containing no nuclei  $n = m + 1$  and for a glass that has sufficiently large nuclei before DTA experiment  $n = m$  [40]. A plot of  $\ln[-\ln(1-\chi)]$  versus  $(1000/T_g)$   $K^{-1}$  data for the studied samples measured at different heating rates shown in Figs.10 (a,b). It is observed that the plots are linear over a wide temperature range, a break in linearity is seen for all heating rates for the studied samples. This is due to the saturation of the nucleation sites at the final stage of crystallization [41], [42] or to the restriction of crystal growth by small size of the particles [43]. From Figs.10 (a,b) the value of  $m E_c$  was calculated from the slope of the linear regions of the  $\ln[-\ln(1-\chi)]$  versus  $(1000/T_g)$   $K^{-1}$  for all heating rates and given in Table 8.

Eq.(8) written in the following form, at constant temperature:  
 $\ln[-\ln(1-\chi)] = -n \ln \alpha + \text{cons} \quad (9)$

Figs.11 (a,b) show linear plots of  $\ln[-\ln(1-\chi)]$  versus  $\ln \alpha$  at three different fixed temperatures for each sample under consideration. According to Eq. (9), the slope of each line in Fig.11 gives the  $n$ -value and hence the value of  $m$  for the studied samples. The values of  $n$  and  $m$  are given in Table 8, since our samples are as-quenched the value of  $n = 4$  and  $m = 3$  for  $Se_{85}Te_{10}In_5$  sample, indicating bulk nucleation with three-dimensional growth. For amorphous  $Se_{85}Te_{10}Sn_5$  Sample, the values of  $n = 3$  and  $m = 2$  indicating the bulk nucleation with two-dimensional growth.

The obtained values of activation energy of crystallization  $E_c$  for the studied samples calculated by different methods are in agreement with each other. It is observed also a considerable difference in the values of  $E_c$  for the studied samples evaluated by different methods. This may be due to different approximations that have been adopted to arrive at the final equation of the various methods.

### 3.3 Thermal stability of glassy alloys

The study of thermal stability and glass forming tendency (GFT) is an important condition for utilizing of chalcogenide glasses as recording materials. These materials exhibit the amorphous - crystallization phase transformation that is utmost importance for the development of some new chalcogenide glasses as better phase change recording materials. Also, the memory and switching materials demand the thermal stability and the ease of glass formation.

Glass forming tendency (GFT) is the relative ability of the glass composition to conform to and remain in the amorphous state. Many studies have done for evaluating GFT and thermal stability of glasses [44], using the ratio  $T_g/T_m$ . Dietzel [45] introduced that the difference between  $T_c$  ( $T_c$  here is the onset temperature of crystallization) and  $T_g$  is a strong indicator of both GFT and thermal stability and is often an important parameter to evaluate the GFT. The higher values of  $T_c - T_g$  the greater the values of GFT. Higher value of  $T_c - T_g$  delays the nucleation process [46]. The

values of  $T_c - T_g$  for a-  $Se_{85}Te_{10}In_5$  and a-  $Se_{85}Te_{10}Sn_5$  samples given in Tables 2 and 3 at different heating rates.

The reduced glass transition temperature for the studied samples is calculated to determine the ease of glass formation according to the relation [44]

$$T_{rg} = T_g / T_m \quad (10)$$

The obtained values of  $T_{rg}$  at different heating rates given in Tables 2 and 3. The average values of the reduced glass transition temperature  $T_{rg}$  are 0.279 and 0.297 for  $Se_{85}Te_{10}Sn_5$  and  $Se_{85}Te_{10}In_5$  compositions respectively, which indicated that the addition of In to Se - Te alloy leads to the ease of glass formation. Hruby [47] calculated the parameter  $H_r$  (Hruby number that is used as an indicator of glass forming tendency GFT. Good GFT is found for glasses with  $H_r \geq 0.4$ ) by the aid of the following relation:

$$H_r = (T_c - T_g) / (T_m - T_p) \quad (11)$$

The thermal stability parameters is also defined in literature [48] by the following expression:

$$H' = \Delta T / T_g \text{ and } S = [(T_p - T_c) / T_g] (T_p - T_g) \quad (12)$$

The higher values of  $S$ , reflect the greater thermal stability of the glass.

The above equations (11&12) applied in the present study to the alloys  $Se_{85}Te_{10}In_5$  and  $Se_{85}Te_{10}Sn_5$ . The values of  $\Delta T$ ,  $H_r$ ,  $H'$  and  $S$  given in Tables 2& 3. It observed from these tables that the highest values of Hruby number  $H_r$ ,  $H'$  and  $S$  are for  $Se_{85}Te_{10}Sn_5$  composition. Therefore,  $Se_{85}Te_{10}Sn_5$  composition can be taken as the most stable in comparison with  $Se_{85}Te_{10}In_5$ .

## 4 CONCLUSION

DTA technique has been used to study the glass transition region and the crystallization kinetics in the chalcogenide glasses  $Se_{85}Te_{10}X_5$  ( $X=In$  or  $Sn$ ) at different heating rates. The analysis of experimental results is carried out by using three different methods under non-isothermal condition. The activation energy for glass transition  $E_g$  and the activation energy for crystallization  $E_c$  obtained for each treatment with close agreement implying the validity of these methods for determination of  $E_g$  and  $E_c$  in the present compositions. The values of Avrami index  $n$  for the studied compositions are found to be 4 for  $Se_{85}Te_{10}In_5$ , which indicates three-dimensional growth, and  $n=3$  for  $Se_{85}Te_{10}Sn_5$  composition which indicating two-dimensional growth. The thermal stability parameters, the Hruby number  $H_r$ , the glass formation tendency (GFT), the temperature difference ( $T_c - T_g$ ), the reduced glass transition temperature  $T_{rg}$  and the thermal stability  $S$  studied as a function of heating rates. Results indicate that the  $Se_{85}Te_{10}Sn_5$  is the better thermally stable glass composition.

Table 1  
EDX for  $Se_{85}Te_{10}Sn_5$  and  $Se_{85}Te_{10}In_5$  films in powder Form

Calculated composition	At % (observed)				Nominal compositions
	Se	Te	Sn	In	
$Se_{85}Te_{10}Sn_5$	80.55	12.77	6.68	-	$Se_{80.55}Te_{12.78}Sn_{6.68}$
$Se_{85}Te_{10}In_5$	81.01	10.23	-	8.76	$Se_{81}Te_{10.23}In_{8.76}$

Table 2  
Heating rate dependence of the characteristic transition temperatures and thermal stability parameters for amorphous  $Se_{85}Te_{10}Sn_5$  composition.

Heating rate $B, ^\circ C/min$	$T_g, ^\circ C$	$T_c, ^\circ C$	$T_p, ^\circ C$	$T_m, ^\circ C$	$\Delta T, ^\circ C (T_c - T_g)$	$H_r$	$H$	$S, ^\circ C$	$T_{18}$
10	60	102	116	238	42	0.344	0.7	13.076	0.252
20	67	114	126	245	47	0.409	0.701	10.567	0.273
30	71	119	136	248	48	0.466	0.676	15.56	0.287
40	72	124	142	247	52	0.495	0.722	17.5	0.292
50	73	131	153	252	58	0.604	0.795	24.109	0.290

Table 3  
Heating rate dependence of the characteristic transition temperatures and thermal stability parameters for amorphous  $Se_{85}Te_{10}In_5$  composition.

Heating rate $B, ^\circ C/min$	$T_g, ^\circ C$	$T_c, ^\circ C$	$T_p, ^\circ C$	$T_m, ^\circ C$	$\Delta T, ^\circ C (T_c - T_g)$	$H_r$	$H$	$S, ^\circ C$	$T_{18}$
10	65	69	85	238	4	0.026	0.062	4.92	0.273
20	70	82	92	242	12	0.081	0.171	3.14	0.289
30	69	80	90	239	11	0.074	0.159	3.04	0.288
40	75	87	99	247	12	0.081	0.16	3.84	0.303
50	83	89	104	251	6	0.041	0.072	3.795	0.330

Table 4  
Values of bond energy values for bonds in  $Se_{85}Te_{10}Sn_5$  and  $Se_{85}Te_{10}In_5$  glasses

Bond	Bond energy kJ/ mole
Se - Se	189.22
Te - Te	142.35
Se - Te	187.57
Se - Sn	176.65
Te - Sn	144.75
Se - In	183.86
Te - In	145.47

Table 5  
Values of  $E_g$  for  $Se_{85}Te_{10}Sn_5$  and  $Se_{85}Te_{10}In_5$  glasses.

Model	$E_g, kJ/mol$	
	$Se_{85}Te_{10}Sn_5$	$Se_{85}Te_{10}In_5$
Kissinger	106.82	74.77
Augis and Bennett	109.63	77.65
Mahadevan et al.	112.45	80.54
Matusit and Sakka	A = 314.71 B = 8.25	A = 314.59 B = 9.45

Table 6  
Values of  $E_c$  for  $Se_{85}Te_{10}Sn_5$  and  $Se_{85}Te_{10}In_5$  glasses.

Model	$E_c, kJ/mol$	
	$Se_{85}Te_{10}Sn_5$	$Se_{85}Te_{10}In_5$
Kissinger	53.40	79.91
Augis and Bennett	56.78	82.96
Mahadevan et al.	60.16	86.02
Matusit and Sakka	A = 336.06 B = 21.94	A = 332.2 B = 10.68

Table 7  
Values of  $K_o$  for  $Se_{85}Te_{10}Sn_5$  and  $Se_{85}Te_{10}In_5$  glasses.

Model	$K_o, S^{-1}$	
	$Se_{85}Te_{10}Sn_5$	$Se_{85}Te_{10}In_5$
Kissinger	$6.5 \times 10^{14}$	$5.94 \times 10^7$
Augis and Bennett	$4.3 \times 10^{14}$	$1.8 \times 10^{11}$
Mahadevan et al.	$6.39 \times 10^{17}$	$1.77 \times 10^{12}$

**Table 8**  
 Values of  $n_c$  and  $m_c$  for  $Se_{85}Te_{10}Sn_5$  and  $Se_{85}Te_{10}In_5$  glasses

Composition	$E_c$ (kJ/mol)	$n_c$	$m_c$	$E_c m_c$
$Se_{85}Te_{10}Sn_5$	56.78	3	2	113.56
$Se_{85}Te_{10}In_5$	82.96	4	3	248.89

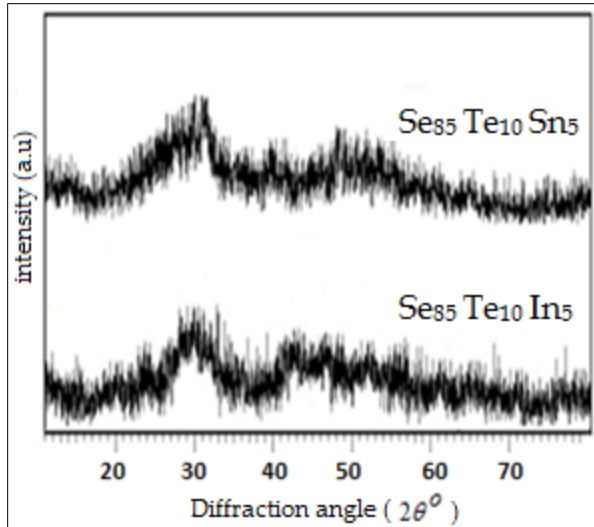
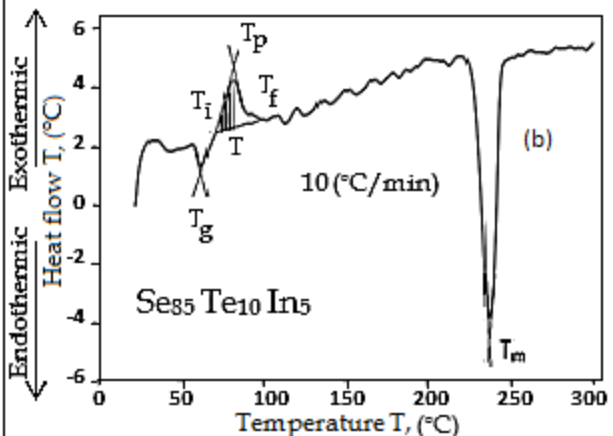
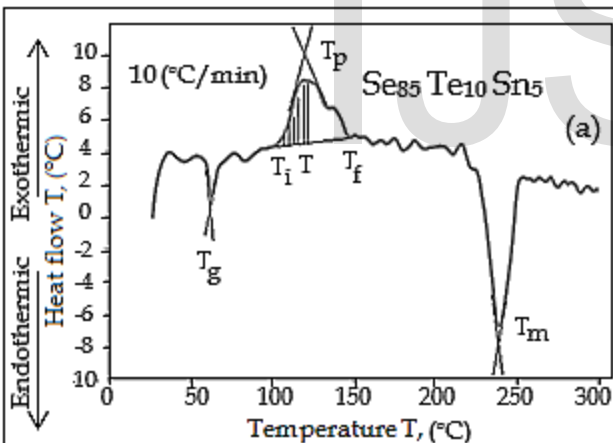
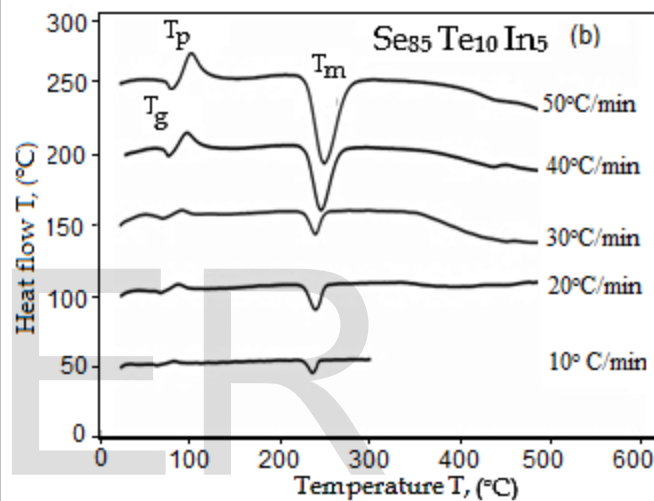
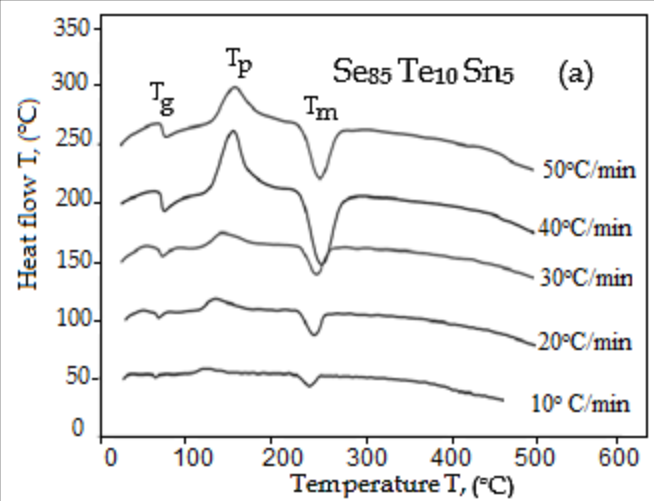


Fig. 1. X-ray diffraction patterns for  $Se_{85}Te_{10}Sn_5$  and  $Se_{85}Te_{10}In_5$  glasses in powder form.



Figs. 2(a,b). Typical DSC trace of  $Se_{85}Te_{10}Sn_5$  and  $Se_{85}Te_{10}In_5$  glasses at a constant heating rate ( $10^\circ C/min$ )



Figs. 3(a,b). A typical DSC trace of  $Se_{85}Te_{10}Sn_5$  and  $Se_{85}Te_{10}In_5$  at different heating rates

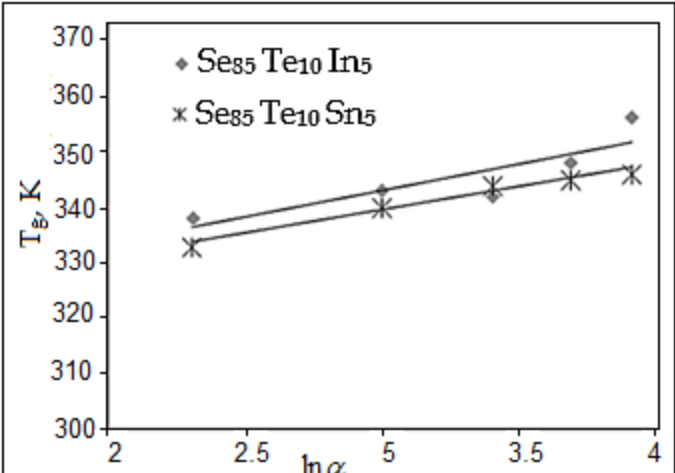


Fig. 4. Plots of  $T_g$  versus  $\ln \alpha$  for  $Se_{85}Te_{10}Sn_5$  and  $Se_{85}Te_{10}In_5$  glasses

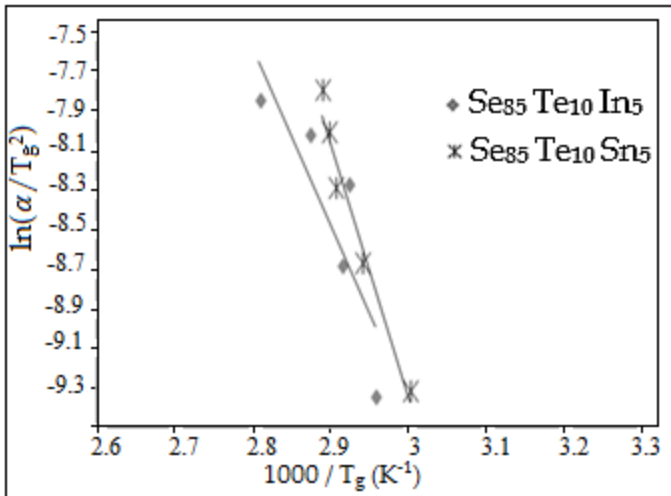


Fig. 5. Variation of  $\ln(\alpha/T_g^2)$  against  $1/T_g$  according to Kissinger formula for  $Se_{85}Te_{10}Sn_5$  and  $Se_{85}Te_{10}In_5$  glasses

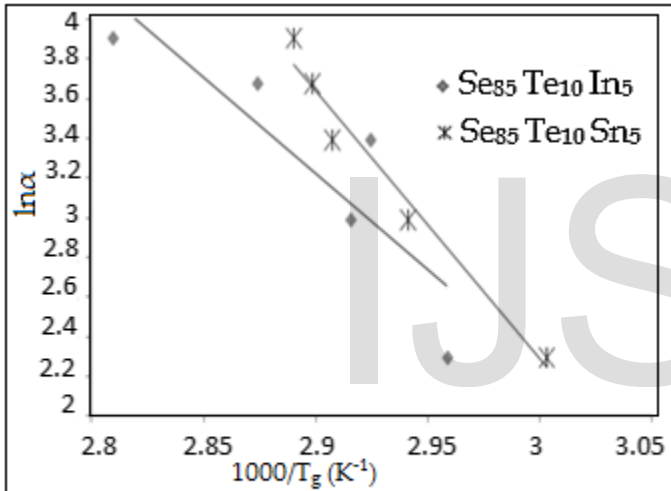


Fig. 6. Variation of  $\ln\alpha$  against  $1/T_g$  according to Mahadevan et al. approximation for  $Se_{85}Te_{10}Sn_5$  and  $Se_{85}Te_{10}In_5$  glasses

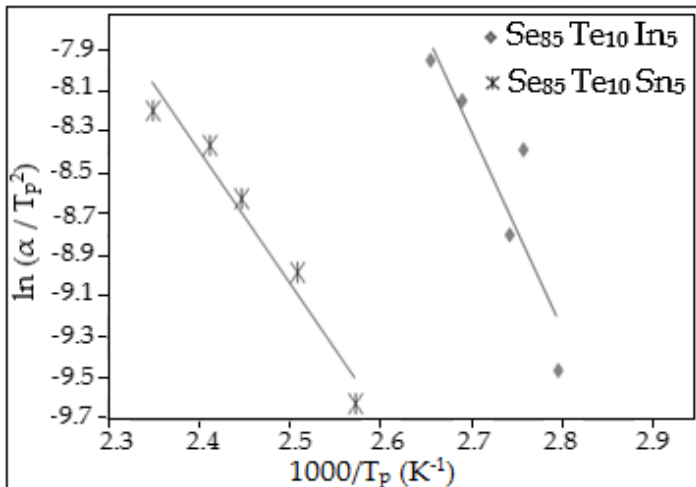


Fig. 7. Variation of  $\ln(\alpha/T_p^2)$  against  $1/T_p$  according to Kissinger formula for  $Se_{85}Te_{10}Sn_5$  and  $Se_{85}Te_{10}In_5$  glasses

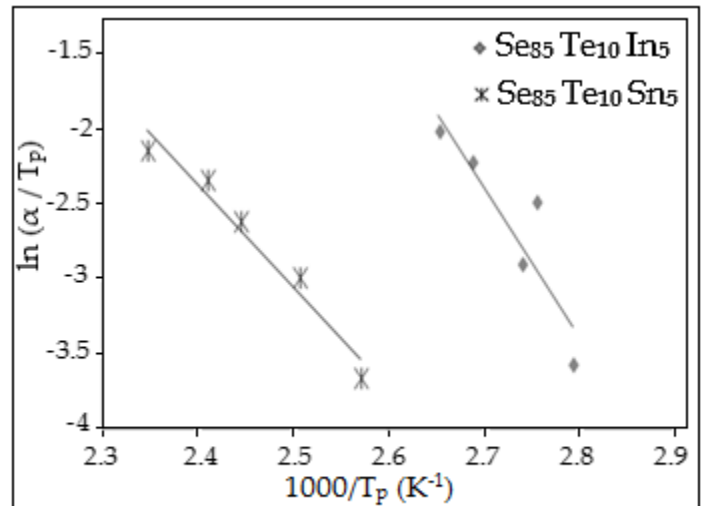


Fig. 8. Plots of  $\ln(\alpha/T_p)$  versus  $1000/T_p$  for  $Se_{85}Te_{10}Sn_5$  and  $Se_{85}Te_{10}In_5$  glasses

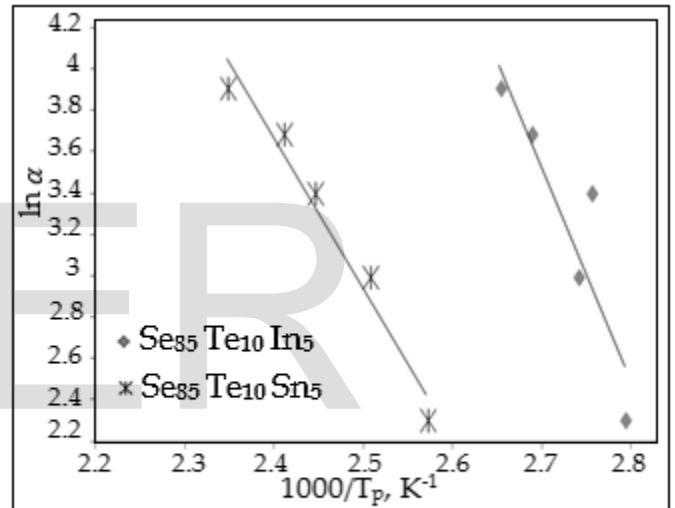
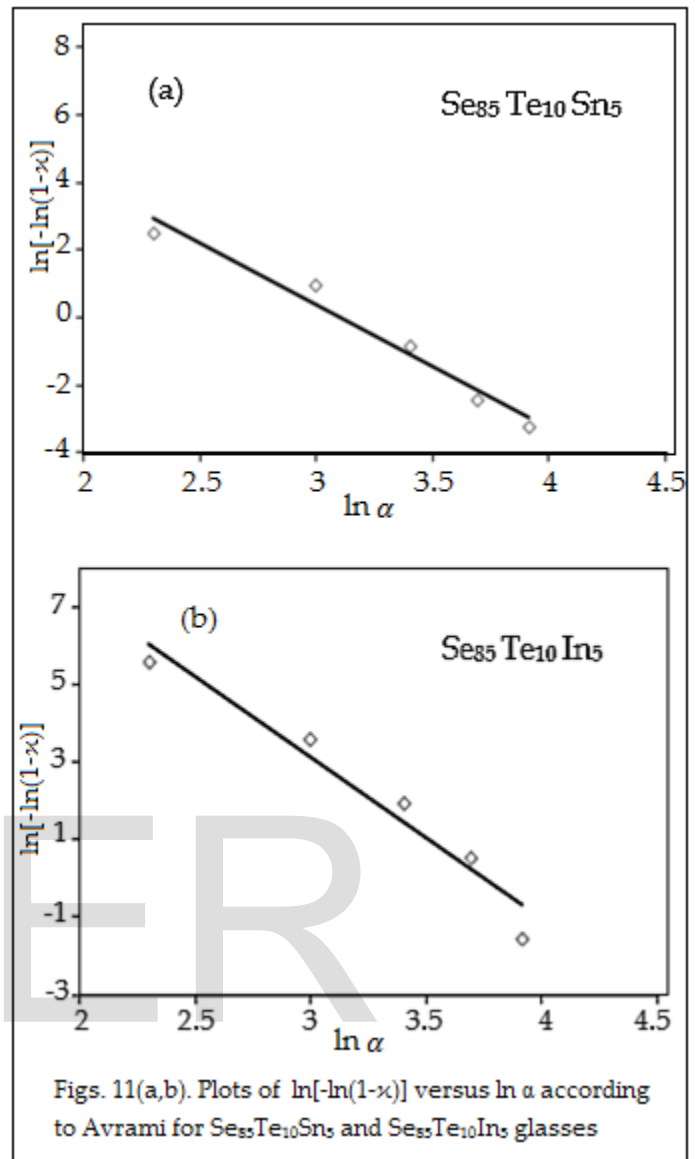
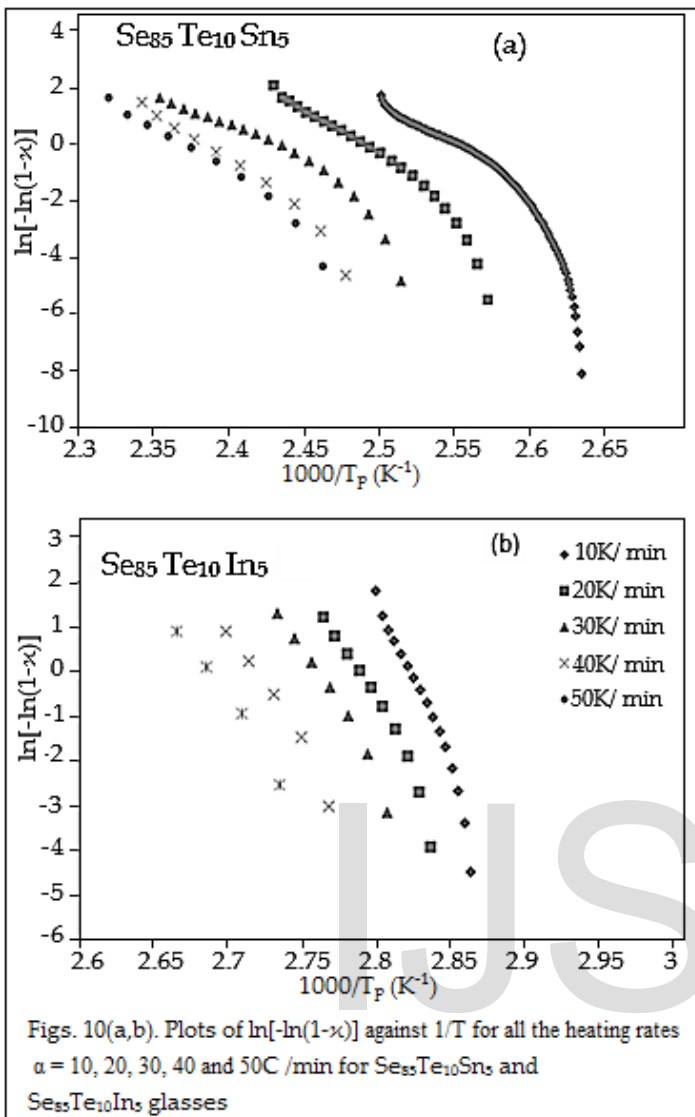


Fig. 9. Variation of  $\ln\alpha$  against  $1000/T_p$  according to Mahadevan et al. approximation for  $Se_{85}Te_{10}Sn_5$  and  $Se_{85}Te_{10}In_5$  glasses



## REFERENCES:

- [1] E. Maruyama, "Amorphous Built-in-Field Effect Photoreceptors," *Jpn. J. Applied Physics*, vol. 21, no. 2, pp. 213, 1982.
- [2] J. Troles, V. Shiryayev, M. Churbanov, P. Houizot, L. Brilland, F. Desevedavy, F. Charpentier, T. Pain, G. Snopatin, J.L. Adam, "GeSe4 Glass Fibres with Low Optical losses in the Mid-IR," *J. Optical Material*, vol. 32, pp. 212, 2009.
- [3] B. Hyot, L. Poupinet, V. Gehanno, P.J. Desre, "Analysis of Writing and Erasing Behaviours in Phase Change Materials," *J. Magnetism and Magnetic Materials*, vol. 249, pp. 504, 2002.
- [4] M. Saxena, "A Crystallization Study of Amorphous  $\text{Te}_x(\text{Bi}_2\text{Se}_3)_{1-x}$  Alloys with Variation of the Se Content," *J. Physics D: Applied Physics*, vol. 38, pp. 460, 2005.
- [5] Yu. Plevachuk, "Electrical Conductivity Measurements for Immiscible In-Se-Te alloys," *J. Alloys Compound*, vol. 288, pp. 151-154, 1999.
- [6] R.M. Mehra, A. Ganjoo, P.C. Mathur, "Electrical and optical properties of  $(\text{Se}_{0.7}\text{Te}_{0.3})_{100-x}\text{In}_x$  system," *J. Applied Physics*, vol. 75, pp. 7339-7334, 1994.
- [7] V. Sharma, A. Thakur, N. Goyal, G.S.S. Saini, S.K. Tripathi, "Effect of In Additive on the Electrical Properties of Se-Te Alloy," *J. Semiconductor Science and Technology*, vol. 20, pp. 103-107, 2005.
- [8] M.A. Inrnan, D. Bhandari, N.S. Saxena, "Glass Transition Phenomena, Crystallization Kinetics and Thermodynamic Properties of Ternary  $\text{Se}_{80}\text{Te}_{20-x}\text{In}_x$  ( $x=2, 4, 6, 8$  and  $10$ ) Semiconducting Glasses: Theoretical and Experimental Aspects," *J. Materials Science and Engineering: A*, vol. 292, pp. 56, 2000.
- [9] K. Singh, N.S. Saxena, "Temperature dependence of thermophysical properties of  $\text{Se}_{80}\text{Te}_{10}\text{In}_{10}$  chalcogenide glass," *J. Materials Science and*



- Engineering: A, vol. 392, pp. 38–41, 2005.
- [10] K. Singh, N.S. Saxena, "Thermal Properties of Neutron Irradiated  $\text{Se}_{80}\text{Te}_{10}\text{In}_{10}$  Glass," *J. Materials Science and Engineering: A*, vol. 346, pp. 287–291, 2003.
- [11] N.S. Saxena, M.A. Mousa Imran, K. Singh, "Simultaneous Measurements of Thermal Conductivity and Diffusivity of  $\text{Se}_{80}\text{Te}_{20-x}\text{In}_x$  ( $x = 2, 4, 6$  and  $10$ ) Chalcogenide Glasses at Room Temperature," *J. Bulletin of Materials Science*, vol. 25, pp. 241–245, 2002.
- [12] N.B. Maharjan, K. Singh, N.S. Saxena, "Calorimetric Studies in  $\text{Se}_{75}\text{Te}_{25-x}\text{Sn}_x$  Chalcogenide Glasses," *J. Physica Status Solidi (a)*, vol. 195, pp. 305–310, 2003.
- [13] N. Goyal, Z. Abdolali, S.K. Tripathi, "Effect of Silver Dissolution on Electrical Properties of  $\text{As}_2\text{S}_3$ ," *J. Materials Science: Materials in Electronics*, vol. 12, pp. 523–526, 2001.
- [14] A. Kumar, M. Hussain, S. Swamp, A.N. Nigam, A. Kumar, "Structural Studies of Glassy Semiconducting  $\text{Se}_{80-x}\text{Te}_{20}\text{In}_x$  Alloys," *J. X-ray Spectrometry*, vol. 19, pp. 243–245, 1990.
- [15] R.M. Mehra, A. Ganjoo, G. Kaur, P.C. Mathur, "Effect of in Impurity on Crystallization Kinetics of  $(\text{Se}_7\text{Te}_3)_{100-x}\text{In}_x$  System," *J. Thermal Analysis and Calorimetry*, vol. 45, pp. 405–415, 1995.
- [16] A.B. Giridhar, J.K. Zope, "Electrical Properties of the Amorphous Semiconducting  $\text{Se Te In}$  System," *J. Non-Crystalline Solids*, vol. 103, pp. 295–299, 1988.
- [17] A. Kumar, A.S. Mann, D.R. Goyal, A. Kumar, "Photoconductivity in Thin Films of  $\text{A-In}_{40}\text{Se}_{30}\text{Te}_{30}$ ," *Jpn. J. Applied Physics*, vol. 27, pp. 1881–1884, 1988.
- [18] H.E. Kissinger, "Reaction Kinetic in Differential Thermal Analysis," *J. Analytical Chemistry*, vol. 29, pp. 1702, 1957.
- [19] K. Matusita, S. Sakka, "Kinetics Study of the Crystallization of Glass by Differential Scanning Calorimetry," *J. Physics and Chemistry of Glasses*, vol. 20, pp. 81, 1979.
- [20] J. A. Augis, J. E. Bennett, "Calculation of the Avrami parameters for Heterogeneous Solid State Reactions Using A Modification of the Kissinger Method," *J. Thermal Analysis and Calorimetry*, vol. 13, pp. 283, 1978.
- [21] P.K. Deepika, K.S. Jain, Rathore, N.S. Saxena, "Structural Characterization and Phase Transformation Kinetics of  $\text{Se}_{38}\text{Ge}_{42-x}\text{Pb}_x$  ( $x = 9, 12$ ) Chalcogenide Glasses," *J. Non-Crystalline Solids*, vol. 355, pp. 1274, 2009.
- [22] M.K. El- Mously, M.M. Zaidia, "Thermal and Electrical Conductivities During the Devitrification of  $\text{Te Se}_{125}$  Amorphous Alloy," *J. Non-Crystalline Solids*, vol. 27, pp. 265, 1978.
- [23] A-Giridhar, S. Mahadevan, "The  $T_g$  Versus  $Z$  Dependence of Glasses of the  $\text{Ge In Se}$  System," *J. Non-Crystalline Solids*, vol. 151, pp. 245, 1992.
- [24] M.K. Rabinal, K.S. Sanguuni, E.S.R. Gopal, "Chemical Ordering in  $\text{Ge}_{20}\text{Se}_{80-x}\text{In}_x$  Glasses," *J. Non-Crystalline Solids*, vol. 188, pp. 98, 1995.
- [25] Shamshad A. Khan, M. Zulfequar, M. Husain, "On the Crystallization Kinetics of Amorphous  $\text{Se}_{80}\text{In}_{20-x}\text{Pb}_x$ ," *J. Solid State Communications*, vol. 123, pp. 463, 1000.
- [26] L.J. Pauling, Nature of the Chemical Bond, Cornell university press, New York 1960.
- [27] M. Lasocka, "The Effect of Scanning Rate on Glass Transition Temperature of Splat-cooled  $\text{Te}_{85}\text{Ge}_{15}$ ," *J. Materials Science and Engineering*, vol. 23, pp. 173, 1976.
- [28] S. Faheem Naqvi, Deepika, N. S. Saxena, Kananbala Sharma, D. Bhandari, "Glass-Crystal Transformations in  $\text{Se}_{80-x}\text{Te}_{20}\text{Ag}_x$  ( $x = 0, 3, 5, 7$  and  $9$ ) Glasses," *J. Alloys and Compounds*, vol. 506, pp. 956, 2010.
- [29] S. M. El. Sayed, "Glass Formation and Local Arrangement of Chalcogenide of  $\text{Ga}_{40}\text{Se}_{60}$  and  $\text{Ga}_{33}\text{Se}_{60}\text{Te}_7$ ," *J. Materials Chemistry and Physics*, vol. 78, pp. 262, 2002.
- [30] H. E. Kissinger, "Variation of Peak Temperature with Heating Rate in Differential Thermal Analysis," *J. Research of the National Bureau of Standards*, vol. 57, pp. 217, 1956.
- [31] H.S. Chen, "A Method for Evaluating Viscosities of Metallic Glasses from the Rates of Thermal Transformations," *J. Non-Crystalline Solids*, vol. 27, pp. 257, 1978.
- [32] J.E. Shelby, "Thermal Expansion of Amorphous Metals," *J. Non-Crystalline Solids*, vol. 34, pp. 111, 1979.
- [33] J. Colemenero, J.M. Bara-ndiaran, "Crystallization of  $\text{Al}_{25}\text{Te}_{77}$  Glasses," *J. Non-Crystalline Solids*, vol. 30, pp. 263, 1978.
- [34] J.A. Macmillan, "Kinetics of Glass Transformation by Thermal Analysis. I. Glycerol," *J. Chemical Physics*, vol. 42, pp. 3497, 1965.
- [35] S. Mahadevan, A. Giridhar, A.K. Singh, "Calorimetric Measurements on  $\text{As-Sb-Te}$  Glasses," *J. Non-Crystalline Solids*, vol. 88, pp. 11, 1986.
- [36] M.M. Imran, D. Bhandari and N. S. Saxena, "Enthalpy Recovery During Structural Relaxation of  $\text{Se}_{96}\text{In}_4$  Chalcogenide," *J. Physica B: Condensed Matter*, vol. 293, pp. 394, 2001.
- [37] P. Agarwal, S. Goel, J. S. P. Rai and K. Kumar, "Calorimetric Studies in Glassy  $\text{Se}_{80-x}\text{Te}_{20}\text{In}_x$ ," *J. Physica Status Solidi (a)*, vol. 127, pp. 363, 1991.
- [38] T. Ozawa, "Kinetics of Non-Isothermal Crystallization," *J. Polymer*, vol. 12, pp. 150, 1971.
- [39] K. Matusita, S. Sakka, "Kinetics Study of the Crystallization of Glass by Differential Scanning Calorimetry," *J. Physics and Chemistry of Glasses*, vol. 20, pp. 81–84, 1979.
- [40] K. Matusita, T. Konatsu, R. Yokota, "Kinetics of Non-Isothermal Crystallization Process and Activation Energy for Crystal Growth in Amorphous Materials," *J. Materials Science*, vol. 19, pp. 291, 1984.
- [41] J. Colemenero and J. M. Barrandiran, "The study of transformation kinetics of the amorphous  $\text{Pd Si}$  alloys," *J. Non-Crystalline Solids*, vol. 21, pp. 411, 1976.
- [42] A. K. Singh, K. Singh, "Crystallization Kinetics and Thermal Stability of  $\text{Se}_{98-x}\text{Zn}_2\text{In}_x$  Chalcogenide Glasses," *J. Philosophical Magazine*, vol. 89, pp. 1457, 2009.
- [43] G. Kaur, T. Komatsu, "Crystallization Behavior of Bulk Amorphous  $\text{Se-Sb-In}$  System," *J. Materials Science*, vol. 36, pp. 4531, 2001.
- [44] S. Sakka, J. D. Mackenzie, "Relation between Apparent Glass Transition Temperature and Liquids Temperature for Inorganic Glasses," *J. Non-Crystalline Solids*, vol. 6, pp. 145, 1971.
- [45] A. Dietzel, "Glass structure and glass properties," *J. GlassTech. Ber.*, vol. 22, pp. 41, 1968.
- [46] N. Mehta, R. S. Tiwari, A. Kumar, "Glass Forming Ability and Thermal Stability of Some  $\text{Se-Sb}$  Glassy Alloys," *J. Materials Research Bulletin*, Mater. Res. Bull., vol. 41, pp. 1664, 2006.
- [47] A. Hruby, "Evaluation of Glass-Forming Tendency by Means of DTA," *J. Physica B*, vol. 22, pp. 1187, 1972.
- [48] M. Saad, M. Poulain, "Glass Forming Ability Criteria," *J. Materials Science Forum*, vol. 19, pp. 11, 1987.